Princeton Plasma Physics Laboratory

PPPL-5137

Wall-touching kink mode calculations with the M3D code

J.A. Breslau

July 2015

Prepared for the U.S. Department of Energy under Contract DE-AC02-09CH11466.

Princeton Plasma Physics Laboratory
Report Disclaimers

Full Legal Disclaimer

Trademark Disclaimer

PPPL Report Availability

Princeton Plasma Physics Laboratory:

http://www.pppl.gov/techreports.cfm

Office of Scientific and Technical Information (OSTI):

http://www.osti.gov/scitech/

Related Links:

U.S. Department of Energy

U.S. Department of Energy Office of Science

U.S. Department of Energy Office of Fusion Energy Sciences

Wall-touching kink mode calculations with the M3D code

J.A. Breslau

Princeton Plasma Physics Laboratory, Princeton, NJ, 08542

Abstract

This paper seeks to address a controversy regarding the applicability of the 3D nonlinear extended MHD code M3D [1] and similar codes to calculations of the electromagnetic interaction of a disrupting tokamak plasma with the surrounding vessel structures. M3D is applied to a simple test problem involving an external kink mode in an ideal cylindrical plasma, set out by its critics as a model case for illustrating the nature of transient vessel currents during a major disruption. While comparison of the results with those of the disruption simulation code is complicated by effects arising from the higher dimensionality and complexity of M3D, we verify that M3D is capable of reproducing both the correct saturation behavior of the free boundary kink and the "Hiro" currents arising when the kink interacts with a conducting tile surface interior to the ideal wall.

I. Introduction

The nonlinear extended MHD code M3D [1] has been employed in the simulation of disruptions arising from vertical displacement events in tokamaks including JET, NSTX, and ITER [2-4], with the goal of providing guidance as to the distribution and timing of the accompanying transient currents to be expected in the conducting structures surrounding the plasma, and to the resulting forces. The nature of the simulations is such that these currents and forces occur at the boundary of the computational domain, making the proper choice of boundary conditions especially critical to the reliability of the results. As has historically been typical with magnetofluid codes, the M3D boundary condition includes the prescription that the normal component of the fluid velocity vanish at the wall. It has been argued [5] that this prescription invalidates M3D's (and similar codes') prediction of vessel currents because it would seem to rule out the possibility of the advection of plasma surface currents into the wall as the plasma flows into it. This claim has been tested by applying M3D to an idealized case based on a simplified model of a kink-unstable plasma column used by an early version of the Disruption Simulation Code [6], in order to abstract the essential physics from some of the complications involved in the attempt to model real devices using realistic parameters. In the next section, we describe the kink mode model and published results in detail. In section III, we describe the methodology and results of M3D calculations of the case. Finally, in section IV we draw some conclusions.

II. The Zakharov test problem

The first published test of the 2D (single-helicity) predecessor to the Disruption Simulation Code (DSC), which we will refer to as the Wall Touching Kink code or WTK, considers the problem of a straight cylindrical column of ideal plasma with radius $a = 0.6\,\mathrm{m}$, separated by a perfect vacuum from an ideal cylindrical wall of radius $b = 1$ m, concentric with the plasma. The plasma is initially in a state of ideal MHD equilibrium with a low uniform pressure, a constant safety factor $q_0 = 1$ in the interior

$(r < a)$, and a lower safety factor $q_a = 0.75$ at the plasma-vacuum boundary, resulting in a singular current along this interface. There may or may not also be a cylindrical tile surface present at radius $c = 0.7$ m; when in vacuum, this surface is considered to behave as a perfect insulator (transparent to magnetic diffusion), while any portion that is wetted by (in contact with) plasma behaves as a perfect conductor. This is meant to model the effect of the plasma conducting current across breaks between the otherwise mutually insulated tiles.

The specified plasma equilibrium is unstable to a 1,1 external kink mode, which here serves as a proxy for the type of macroscopic instability that may lead to the thermal quench in a disrupting tokamak. The WTK code tracks the 2D nonlinear evolution of this mode using a Lagrangian formulation in which the numerical mesh adapts to the shape of the plasma and moves with it through the vacuum. The equations solved are a variant of the MHD equations referred to by the code's authors as "tokamak MHD", in which the inertial term in the momentum equation is replaced by a term involving the displacement $\boldsymbol{\xi}$:

$$\rho \frac{d\mathbf{v}}{dt} \rightarrow \gamma \mathbf{v} = \lambda \boldsymbol{\xi} \tag{1.1}$$

for some time-dependent normalization λ, in order to eliminate Alfvén wave physics (considered irrelevant to the mode) from the calculation and enhance its speed. This amounts to an evolving equilibrium description with a drag term that should evolve towards a true equilibrium state in the limit that the velocity vanishes, but rules out the computation of other ideal or linear resistive modes that could become unstable. The calculation thus proceeds until the mode saturates.

In the absence of the tile surface, the mode is a simple free boundary kink. The plasma approaches the ideal wall as it distorts helically until the mirror currents induced there are sufficient to resist any further motion, resulting in a helical saturated state close to the wall (Figure 3 of Ref. [6]).

When the tile surface is present, it is invisible to the disrupting plasma until the plasma makes contact with it, initially at a single poloidal location. At that point there is no hydrodynamic impediment to the continued flow of the simulated plasma into and beyond the tiles, as there would be for a conducting liquid; rather the plasma surface current (which is opposite to the direction of the bulk plasma current in the region in contact with the tiles) is shared with the tiles, and this "Hiro" current exerts an electromagnetic force that slows the plasma motion, assuming the same role played by the wall currents in the free boundary case (Figure 7 of Ref. [6]). The resulting quasi-saturated state within the $r = c$ surface is called the wall-touching kink. It decays on a longer timescale as the plasma is neutralized by contact with the solid tiles.

III. M3D Calculations

3.1 Equilibrium

The many numerical differences between the DSC and WTK codes and M3D necessitate a number of approximations in the reproduction of the test problem in the latter. Because M3D is obligated to work in toroidal geometry, we approximate the straight cylinder as a large-aspect-ratio torus. Because it is an Eulerian, resistive MHD code, we approximate the ideal plasma as one with finite but relatively low resistivity and the vacuum region as a much colder plasma with correspondingly higher resistivity; the boundary between the two is not sharp, but is defined by an evolving threshold value of the pressure. Because M3D represents all fields using finite elements constructed with linear basis functions, the

singular current sheet at the plasma boundary is approximated by a region of small but finite thickness $\delta \ll a$ spanning several mesh zones over which the magnetic field and pressure change rapidly. For simplicity's sake, the plasma density ρ is kept uniform over the entire computational domain and does not evolve in time.

Given a major radius R_0 and on-axis toroidal field B_0, the solution to the Grad-Shafranov equation for the inner region $0 \le r \le a - \delta$ with constant safety factor q_0 and pressure p_0 is

$$RB_\phi(r) = \frac{q_0^2 R_0^2 B_0}{q_0^2 R_0^2 + r^2}, \tag{1.2}$$

$$J_\phi(r) = \frac{2q_0^3 R_0^3 B_0}{\left(q_0^2 R_0^2 + r^2\right)^2}. \tag{1.3}$$

Over the boundary region $a - \delta \le r \le a$ we prescribe that the pressure drops linearly in r with gradient γ to a small but finite value ε:

$$p(r) = p_0 - \gamma\left[r - (a-\delta)\right] = \varepsilon + \gamma(a - r) \tag{1.4}$$

Requiring that q drop to q_a at $r = a$ and that the toroidal field be continuous at $r = a - \delta$, we find that

$$RB_\phi(r) = \frac{q_0^2 R_0^2 B_0}{q_0^2 R_0^2 + (a-\delta)^2} \tag{1.5}$$

and

$$J_\phi(r) = \frac{\gamma r}{\sqrt{\frac{2\gamma\left(r^3 - a^3\right)}{3} + \frac{a^4 B_{b,z}^2}{q_a^2 R_0^2}}} \tag{1.6}$$

in this region, where $B_{b,z}$ is the equivalent constant cylindrical longitudinal field outside the plasma, *i.e.*, the right-hand-side of equation (1.5). Solving for force balance then determines the pressure gradient to be

$$\gamma = \frac{3}{2\left[(a-\delta)^3 - a^3\right]}\left\{\frac{q_0^2 R_0^2 B_0^2 (a-\delta)^4}{\left[q_0^2 R_0^2 + (a-\delta)^2\right]^2} - \frac{a^4 B_{b,z}^2}{q_a^2 R_0^2}\right\}. \tag{1.7}$$

In terms of free parameter $\zeta \equiv p_0 / \varepsilon$, then,

$$\varepsilon = \frac{\gamma\delta}{\zeta - 1} \tag{1.8}$$

and $p_0 = \varepsilon + \gamma\delta$. In the vacuum region $a \le r \le b$, the pressure is once again uniform, the current density vanishes, and for continuity, RB_ϕ assumes the same constant value $B_{b,z}$ it has in the boundary layer. For aspect ratio $R_0 = 72$, relative boundary layer thickness $\delta / a = 0.1$, and pressure ratio $p_0 / \varepsilon = 100$, these prescriptions result in the equilibrium shown in Figure 1. The case shown used 190 mesh zones in the minor radial direction, which proved ample to resolve the boundary layer, at about 8 zones across. By means of a brief two-dimensional (axisymmetric) nonlinear calculation with this state as the initial condition, it was verified that it represents a genuine numerical steady state within M3D.

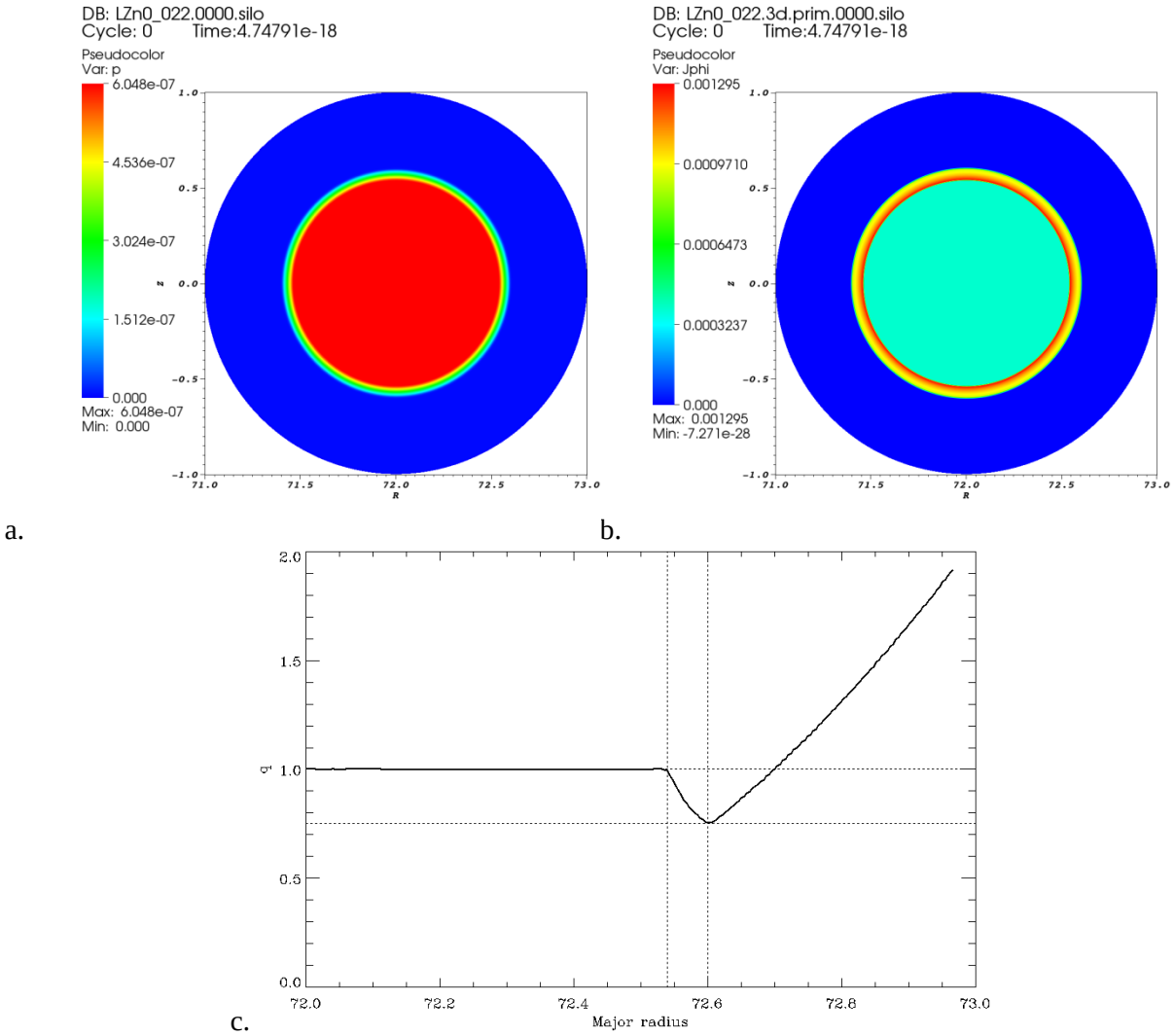

Figure 1: Profiles of the large aspect ratio toroidal M3D equilibrium approximating the ideal cylindrical Zakharov test case. a. Pressure. b. Toroidal current density. c. Safety factor.

3.2 Linear stability

The chosen equilibrium is expected to be unstable to an ideal external kink mode. As a single-helicity code, WTK models this as a rigid helical 1,1 displacement of the plasma column from its equilibrium position at the center of the vessel off axis into the vacuum region, towards the wall. While the lack of a true vacuum – and uniform density – in the M3D model means that this will not be a precise description of its unstable *n*=1 mode (the M3D eigenmode will have displacement in the vacuum region), the WTK mode is nevertheless useful as an initial guess for the linear eigenmode calculation within M3D. Accordingly, we begin that calculation by perturbing the equilibrium stream function *U* for poloidal velocity with a single helicity displacement:

$$U_1(r,\theta,\phi) = \begin{cases} r\xi_{1,1}\sin(\theta-\phi), & 0 \le r \le a \\ 0, & a < r \end{cases} \tag{1.9}$$

M3D is then run in its linear mode until convergence on an *n*=1 mode is reached. We choose a normalized plasma resistivity of $\eta = 10^{-6}$; because M3D has a Spitzer-like dynamic resistivity profile with $\eta \propto T^{-3/2}$ and because $T_{plas}/T_{vac} = p_{plas}/p_{vac} = 100$ for this case, this gives an approximate normalized vacuum resistivity of 10^{-3}. Normalized kinematic viscosity is uniform at $\mu = 10^{-5}$. The mode is found to be unstable with growth rate $\gamma\tau_A \approx 5.8\times10^{-3}$. Its structure is found to resemble the initial perturbation, but with additional flow of the displaced "vacuum" around the plasma column to conserve density (Figure 2).

The Zakharov paper does not address the stability of ideal modes with toroidal mode number $n > 1$. Using the same transport parameters as the above calculation, M3D finds some of these to be unstable as well; there is a 2,2 mode with a growth rate of $\gamma\tau_A \approx 8.3\times10^{-3}$ and a 3,3 mode with $\gamma\tau_A \approx 8.8\times10^{-3}$ (Figure 3). In the limit of large aspect ratio, approaching the straight cylinder case, however, these higher-*n* modes are expected to decouple from the *n*=1; as a result, and for a fair comparison with WTK, we ignore them and initialize our nonlinear calculation with the pure *n*=1 eigenmode.

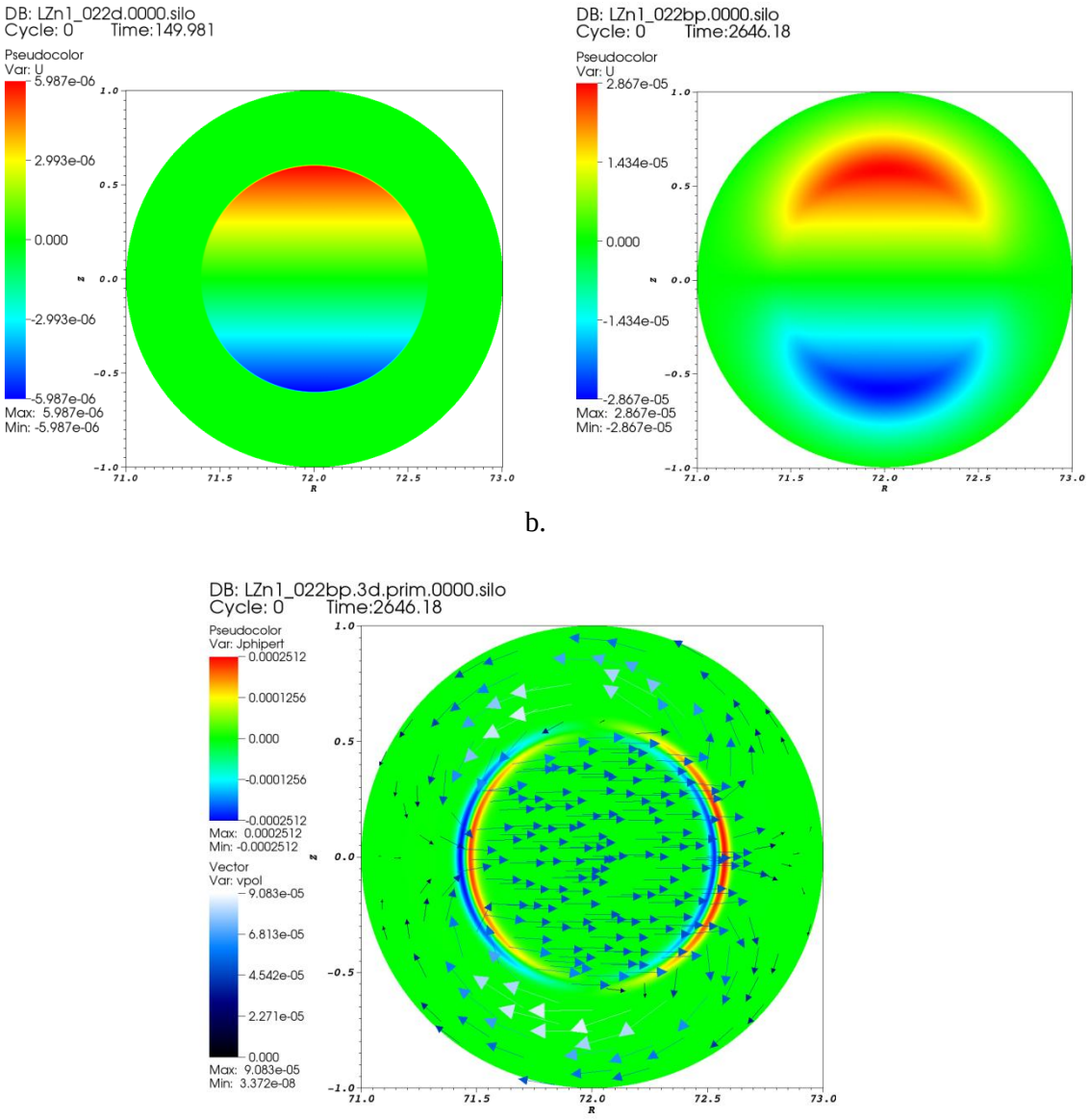

Figure 2: a. Initial *n*=1 perturbation to velocity stream function U in M3D linear eigenmode calculation (plane $\phi = 0$). b. Profile of *U* in converged *n*=1 eigenmode. c. Profile of perturbed toroidal current density J_ϕ (color contours) and poloidal flow pattern (arrows) in *n*=1 eigenmode.

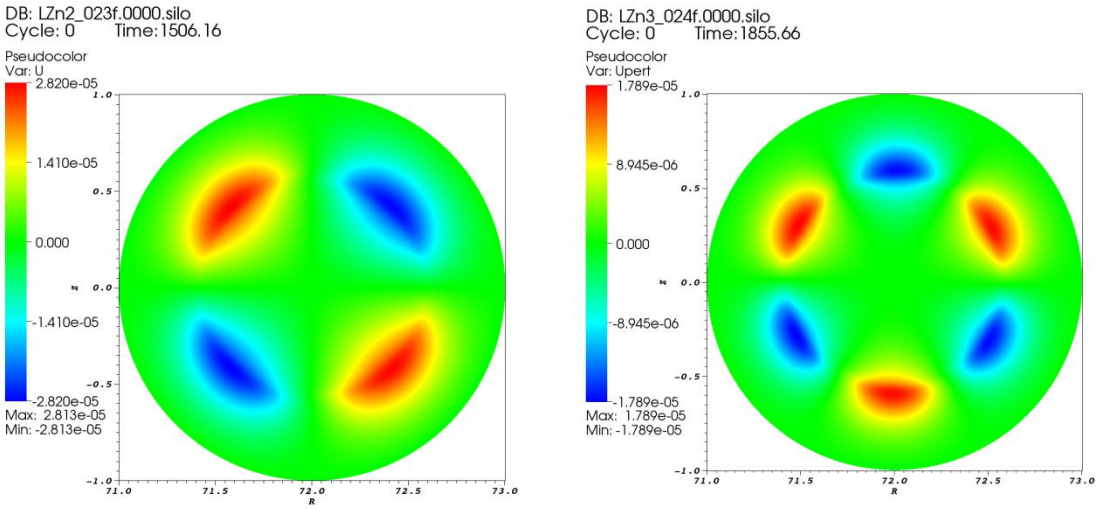

a. b.

Figure 3: Perturbed poloidal velocity stream function U in the $\phi = 0$ plane for unstable n>1 eigenmodes of the aspect-ratio-18 equilibrium. a. n=2. b. n=3.

3.3 Nonlinear free boundary kink

For comparison with the Zakharov free boundary kink result, we first initialize a 3D nonlinear calculation with 64 toroidal planes using the aspect-ratio-72 equilibrium as the initial state, with the previously computed n=1 eigenmode superimposed as a perturbation at sufficient amplitude to bring the initial total kinetic energy to 10^{-9} in normalized units, which is low enough to fall within the linear regime. An ideal wall with the boundary condition $v_{normal}=0$ is present at r=1, but no tile surface is implemented. Resistivity and viscosity within the domain are the same as in the linear calculation; parallel and perpendicular heat conduction coefficients are set to $\kappa_{\|} = 500$ and $\kappa_{\perp} = 10^{-6}$ respectively. An Ohmic heating term is present in the energy equation; aside from this, there are no other sources or sinks.

Results are summarized in Figure 4. During the initial, linear phase of the instability, the behavior of the mode closely resembles that reported by Zakharov, *et al.*: there is a rigid helical displacement of the plasma column toward the ideal wall. As the column approaches the wall more closely, it begins to deform into a D shape very similar to that visible in Fig. 1c. At about the time of saturation (peak n=1 kinetic energy at $t \approx 3150$), however, another phenomenon is observed: a bubble of vacuum begins to make its way into the plasma, distorting it first into a crescent and finally an annulus. The intrusion of the vacuum bubble appears to be generic, occurring for a wide variety of aspect ratios and run parameters, and we believe it to be a genuine physical effect arising from the flat rational q profile, as explained in Ref. [7].

A point to note is that, contrary to the Zakharov picture, in which the linear n=1 surface current is oppositely directed to that of the bulk plasma in its direction of motion, here the initial perturbed toroidal current density profile contains components of both signs, nearly equal and opposite to each other. This agrees with recent analytic work by C.-S. Ng [8]. In the late nonlinear phase, however, the surface current nearest the wall is clearly negative with respect to that of the bulk plasma, as in the WTK result.

a.

	Resistivity	Net toroidal current density	Perturbed toroidal current density
t = 2700	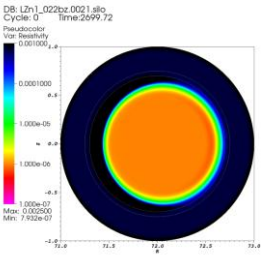	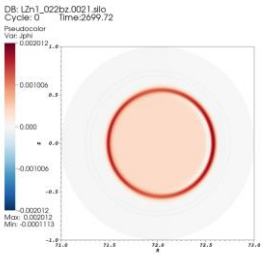	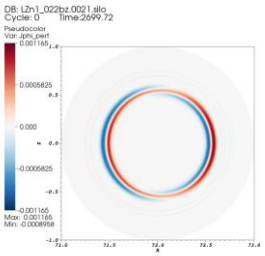
t = 2900	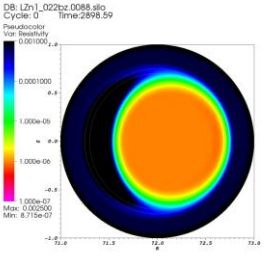	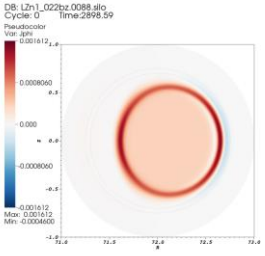	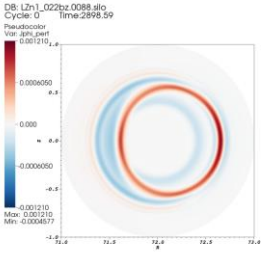
t = 3000	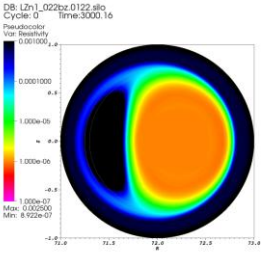	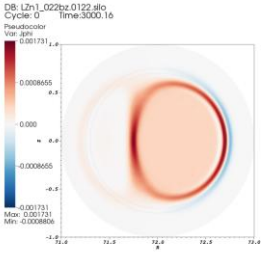	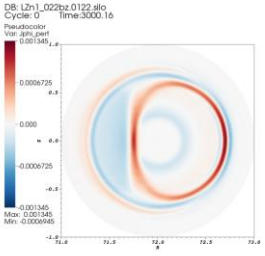
t = 3100	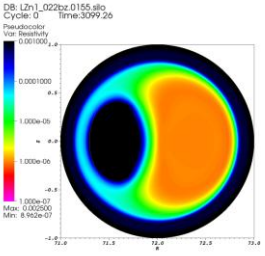	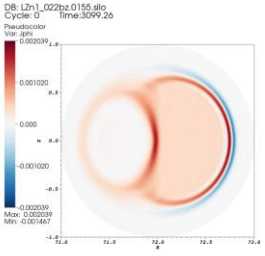	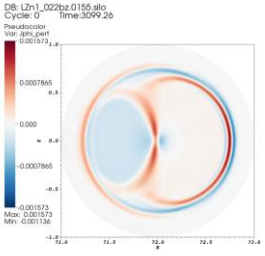
t = 3400	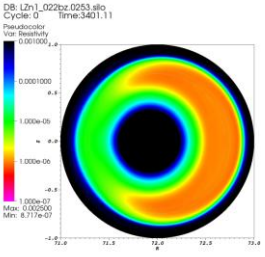	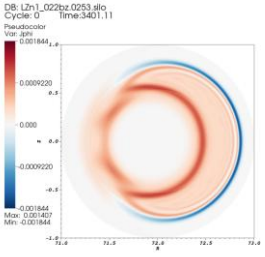	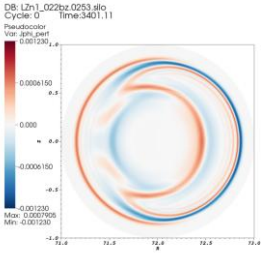

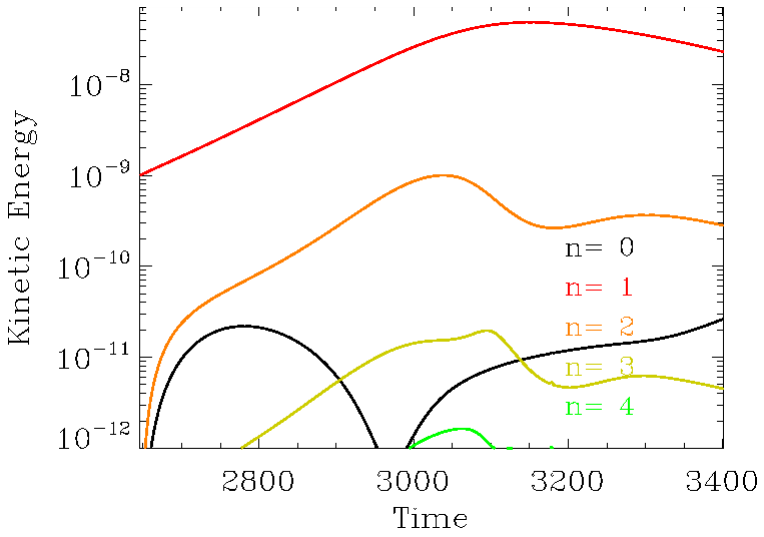

b.

Figure 4: Nonlinear M3D results for the free boundary kink. a. Snapshots of resistivity, toroidal current density, and perturbed toroidal current density profiles in the $\phi = 0$ plane at several times during the instability. b. Kinetic energy vs. time broken down by toroidal mode number.

3.4 Wall-touching kink

The key addition to the model in the wall-touching kink case is the tile surface interior to the computational domain. Because M3D cannot resolve a singular current sheet except on the domain boundary, we model the tiles as an annular region extending from $r = c = 0.7$ to $r = c + \delta_{tile}$, where we have here chosen tile thickness $\delta_{tile} = 0.05$. This region behaves as ordinary vacuum, with Spitzer resistivity when not wetted by plasma. It is considered to be wetted only where the pressure

$$p > \frac{p_{\max} + 3p_{\min}}{4}, \tag{1.10}$$

where $p_{\max}$ and $p_{\min}$ are respectively the instantaneous maximum and minimum pressures over the entire domain. Wetted tiles differ from non-wetted tiles in having resistivity $\eta_{tile} \le \eta_{plasma}$, typically in the range $10^{-8} \le \eta_{tile} \le 10^{-6}$, as M3D cannot represent infinite conductivity in interior structures. In addition to the resistivity prescription, there is a "boundary" condition on temperature for the annulus: $T = \varepsilon$ for $r > c + \delta_{tile}$. This is the equivalent of the $T \to 0$ boundary condition imposed in the free boundary case (and M3D in general), and, because the only distinction between plasma and vacuum in M3D is temperature, ensures that plasma is properly neutralized by contact with the wall. There are no special conditions placed on normal or tangential velocity at the tile surface and the region is not constrained to be in force balance.

a.

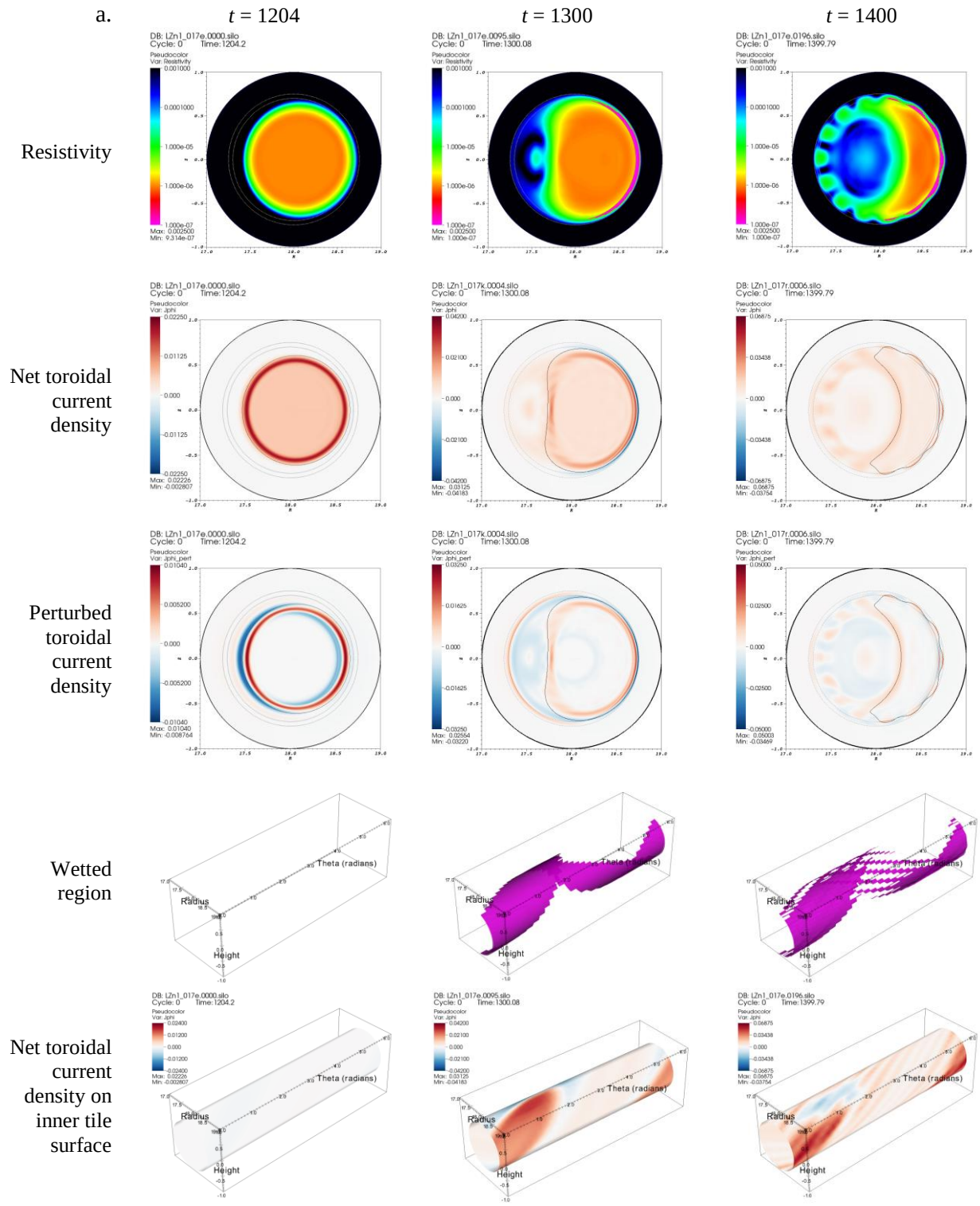
t = 1204
t = 1300
t = 1400
Resistivity
Net toroidal current density
Perturbed toroidal current density
Wetted region
Net toroidal current density on inner tile surface
Theta (radians)
Radius
Height

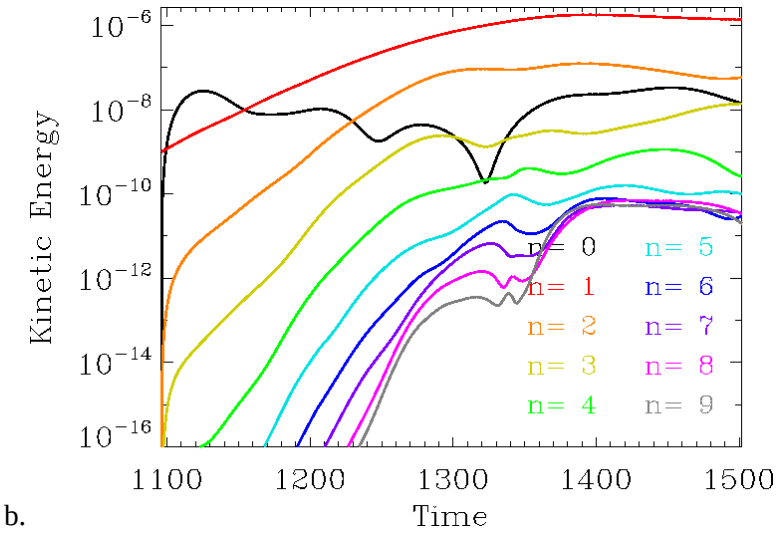

b.

Figure 5: Nonlinear M3D results for the wall-touching kink. a. Snapshots of resistivity, toroidal current density, and perturbed toroidal current density profiles in the $\phi = 0$ plane; and wetted region and tile current around the torus at three times during the instability. b. Kinetic energy vs. time broken down by toroidal mode number.

The nonlinear wall touching kink calculation is initialized identically to the free boundary kink calculation. Results are shown in Figure 5 for an aspect-ratio-18 case with $\eta_{tile} = 10^{-7}$. The lower aspect ratio evidently leads to stronger coupling between neighboring toroidal mode numbers, and more activity seen at higher *n*, but the *n*=1 component remains dominant. Behavior is identical to the equivalent free boundary case until the tile surface is first wetted. The resistivity drop in the surface at that point allows a thin sheet of halo current to flow on an elliptical patch of the helical contact area between the plasma and tiles, slowing the plasma motion and causing mode saturation to begin within the tile surface, at some remove from the ideal wall. The beginning of a vacuum bubble is observed as in the free boundary case, but the plasma disperses on the tiles before it can fully penetrate. At late times some filamentation of the plasma-vacuum boundary occurs, superficially resembling a ballooning mode. As in the free boundary case, the surface currents in the linear eigenmode have two signs at a given poloidal angle, and nearly cancel. Also as in that case, however, the outermost current spike in the late nonlinear phase is negative, and we identify it with the "Hiro" current described in the WTK result.

The nonlinear calculation was repeated with both lower $\left(\eta_{tile} = 10^{-8}\right)$ and higher $\left(\eta_{tile} = 10^{-6}\right)$ values of the tile resistivity. There was no discernible difference in the result, suggesting that the low temperature plays a more important role than the high conductivity of the tile surface in arresting the plasma motion in this simulation.

IV. Conclusions

Using a number of justifiable approximations, the M3D code has proved capable of representing a reasonable facsimile of the ideal straight-cylinder equilibrium with surface current, which was set out as a test case for disruption simulation. Because it solves the full set of time-dependent resistive MHD equations in three dimensions, M3D sees more complex behavior than the idealized saturated kink solution reported by the DSC developers, namely the existence of linearly unstable modes with $n>1$; the present of current sheets of both signs in the $n=1$ eigenmode; and the formation of a vacuum bubble in the nonlinear phase of the instability. This last phenomenon, which is physically correct for an equilibrium with no shear, complicates the comparison between the codes. Nevertheless, both the interaction of the plasma surface currents with the ideal wall in the free boundary kink case and the interaction of the what the authors of [6] call "Hiro currents" with the plasma in the wall-touching kink lead to transient saturated states sufficiently similar to those reported earlier to claim agreement. In M3D as in WTK, the plasma retains finite velocity normal to the tile surface and can penetrate it on a time scale longer than that of the ideal kink. We conclude that, contrary to earlier assertions, the physics model in the M3D code is adequate to accurately predict wall currents arising during disruptions.

It might be argued that the effect of the M3D velocity boundary condition on disruption calculations in which the plasma comes into contact with a resistive first wall at the computational boundary remains unresolved by this study. This is in part the consequence of a lack of adequate test cases for comparison: a DSC result has yet to be published for such a scenario. At any rate, it will be instructive to repeat the wall-touching kink calculation described here, moving the tile wall to the computational boundary and applying M3D's resistive wall boundary condition there. Results to date suggest that the effect of the velocity boundary condition on the sharing of plasma current with the wall will be minor, as the current diffuses in on the wall's resistive time scale regardless of plasma flow.

Acknowledgments

The author gratefully acknowledges useful discussions with Amitava Bhattacharjee, Stephen Jardin, Harry Mynick, Chung-Sang Ng, Hank Strauss, and Leonid Zakharov. This research used resources of the National Energy Research Scientific Computing Center, which is supported by the Office of Science of the U.S. Department of Energy under Contract No. DE-AC02-05CH11231.

References

[1] W. Park, E.V. Belova, G.Y. Fu, X.Z. Tang, H.R. Strauss, and L.E. Sugiyama, *Phys. Plasmas* **6,** 1796 (1999).

[2] H.R. Strauss, R. Paccagnella, and J. Breslau, *Phys. Plasmas* **17**, 082505 (2010).

[3] H. Strauss, R. Paccagnella, J. Breslau, L. Sugiyama, and S. Jardin, *Nucl. Fus*. **53**, 073018 (2013).

[4] H. Strauss, L. Sugiyama, R. Paccagnella, J. Breslau, and S. Jardin, *Nucl. Fus*. **54**, 043017 (2014).

[5] L.E. Zakharov, Phys. Plasmas **17**, 124703 (2010).

[6] L.E. Zakharov, S.A. Galkin, S.N. Gerasimov, and JET-EFDA contributors, Phys. Plasmas **19**, 055703 (2012).

[7] M.N. Rosenbluth, D.A. Monticello, H.R. Strauss, and R.B. White, *Phys. Fluids* **19**, 1987 (1976).

[8] P. Bolgert, CS Ng, J. Breslau, and A. Bhattacharjee, *Bull. Am. Phys. Soc*. **59** (2014).

PPPL PRINCETON PLASMA PHYSICS LABORATORY

Princeton Plasma Physics Laboratory
Office of Reports and Publications

Managed by
Princeton University

under contract with the
U.S. Department of Energy
(DE-AC02-09CH11466)

P.O. Box 451, Princeton, NJ 08543
Phone: 609-243-2245
Fax: 609-243-2751

E-mail: publications@pppl.gov

Website: http://www.pppl.gov